

Emerging applications of stimuli-responsive polymer materials

Martien A. Cohen Stuart, Wilhelm T. S. Huck, Jan Genzer, Marcus Müller, Christopher Ober, Manfred Stamm, Gleb B. Sukhorukov, Igal Szleifer, Vladimir V. Tsukruk, Marek Urban, Françoise Winnik, Stefan Zauscher, Igor Luzinov and Sergiy Minko*

Responsive polymer materials can adapt to surrounding environments, regulate transport of ions and molecules, change wettability and adhesion of different species on external stimuli, or convert chemical and biochemical signals into optical, electrical, thermal and mechanical signals, and vice versa. These materials are playing an increasingly important part in a diverse range of applications, such as drug delivery, diagnostics, tissue engineering and 'smart' optical systems, as well as biosensors, microelectromechanical systems, coatings and textiles. We review recent advances and challenges in the developments towards applications of stimuli-responsive polymeric materials that are self-assembled from nanostructured building blocks. We also provide a critical outline of emerging developments.

To sustain life and maintain biological function, nature requires selectively tailored molecular assemblies and interfaces that provide a specific chemical function and structure, and which change in their environment. Synthetic polymer systems (Fig. 1) with very similar attributes are often prepared for a broad range of applications, such as responsive biointerfaces that are functionally similar to natural surfaces¹; controlled drug-delivery and release systems^{2–4}; coatings that are capable of interacting with and responding to their environment^{5–7}; composite materials that actuate and mimic the action of muscles⁸; and thin films and particles that are capable of sensing very small concentrations of analytes^{9,10}.

This article focuses on stimuli-responsive macromolecular nanostructures that are capable of conformational and chemical changes on receiving an external signal. These changes are accompanied by variations in the physical properties of the polymer. The signal is derived from changes in the materials' environment, such as a change in temperature, chemical composition or applied mechanical force, or that can be triggered exogenously by irradiation with light or exposure to an electrical and magnetic field. Here we analyse only the very recent developments (that is, in the past five years) on the route to applications using stimuli-responsive nanostructured polymer materials and systems in thin films and nanoparticles; the systems covered are summarized in Fig. 1. We discuss two-dimensional (2D) (films) and three-dimensional (3D) (particulates and their assemblies) stimuli-responsive systems from different architectures and fundamental approaches in the area of responsive materials. We then look at how these fundamental approaches to inducing stimuli-responsiveness in each type of system can be used for applications. Finally, challenges in theory and modelling of these complex systems and future prospectives are examined.

Reconstructable surfaces and applications

Reconstructable surfaces change their wettability and permeability, as well as their adhesive, adsorptive, mechanical and optical properties. Emerging applications extend to materials with rapidly switchable adhesion to interacting materials (from sticky to non-sticky surfaces) and wetting (from wettable to non-wettable), with switchable appearance and transparency, and coatings capable of rapid release of chemicals, as well as self-healing coatings.

Principal architectures and mechanisms. Reconstructable surfaces fall into several categories: (1) polymer surfaces formed spontaneously in bulk polymer materials; (2) grafted polymer thin films (here referred to as polymer brushes); (3) thin films of polymer networks; and (4) self-assembled multilayered thin films. In comparing different architectures one should consider dynamics (rate of response) and amplitude of changes of the materials' properties, reversibility of the changes and the intensity of the external signal that could trigger the changes.

Surface reconstruction of bulk polymers often results in long response times (minutes to tens of hours), during which various polymer constituents either migrate to the surface from the bulk or rearrange locally and decrease the interfacial tension^{11,12}. The duration of that response is too slow for many applications. A rapid response with no corruption of the mechanical properties of the bulk material can be achieved through a thin polymer-film coating. By using new design techniques, response times in thin films can now be tuned smoothly from seconds to hours.

A specific example of stimuli-responsive thin films involves macromolecules that are grafted chemically to a surface at sufficiently high grafting densities so that the polymer chains experience excluded volume repulsions and adopt a stretched conformation (that is, polymer brushes, Fig. 2a–c)⁶. The behaviour of polymer brushes is dictated by a combination of strong entropic repulsion between polymer chains in the crowded monolayer, entropic stretching costs and frozen constraints owing to irreversible grafting.

The discovery of reversible switching by external stimuli in polymer brushes — which were prepared either through the 'grafting to' approach^{13,14} or the 'grafting from' approach^{15–20} — has offered exciting possibilities for the fabrication of adaptive and responsive interfaces. Uniform^{13–16,18}, patterned¹⁷ and gradient brushes (brushes in which grafting density and/or chemical composition gradually changes in one or two directions on the surface of the sample)^{6,19,20} have been used to generate responsive films on planar^{13,15–20} and curved (for example, nanoparticle^{6,14}) surfaces.

For single-component homopolymer brushes (Fig. 2a), responsive behaviour originates from the properties of the grafted polymer chains and their grafting densities. Various changes in the environment of the brushes were used to trigger the reconstruction of and change in the brush properties. For example,

*A full list of authors and their affiliations appears at the end of the paper.

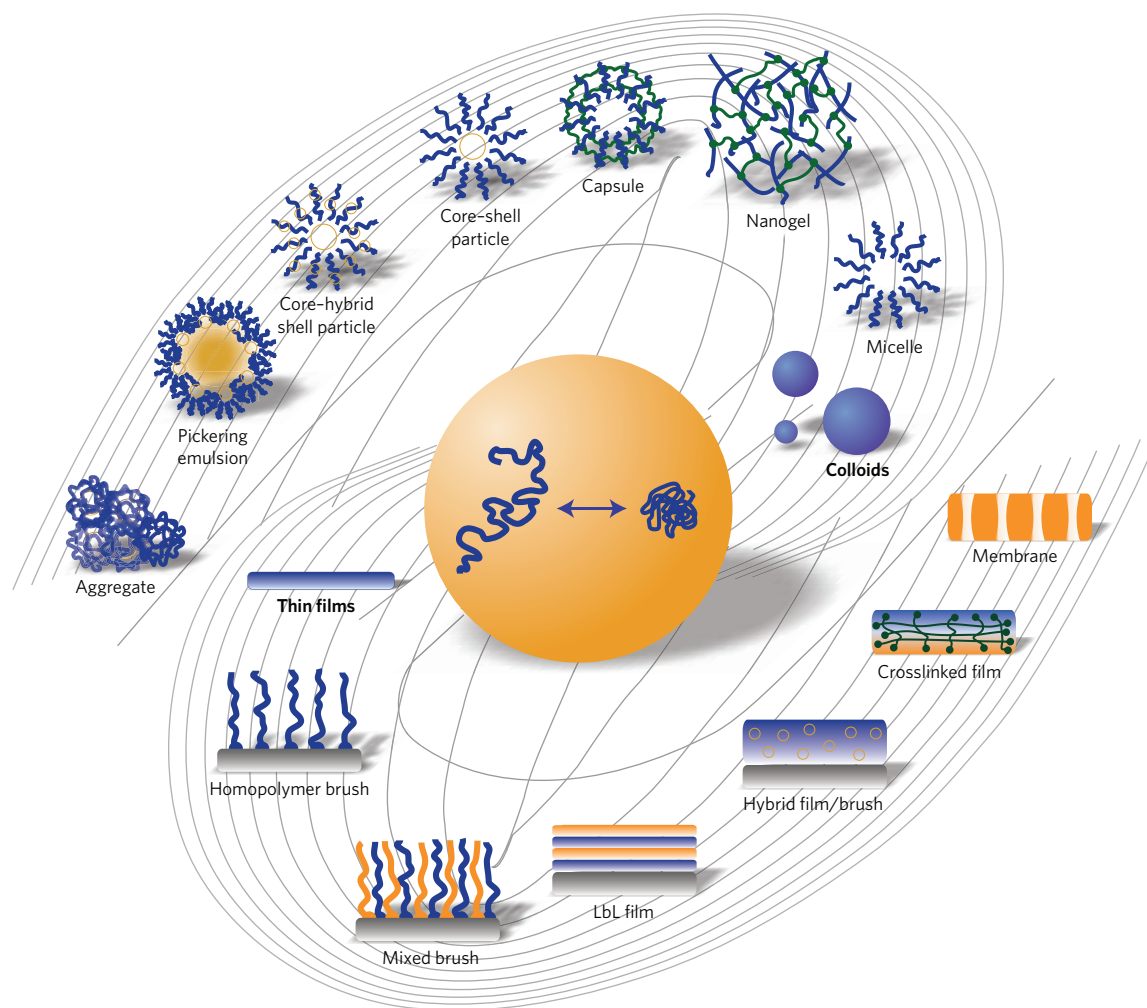


Figure 1 | 'Galaxy' of nanostructured stimuli-responsive polymer materials. These materials rely on the phase behaviour of macromolecule assemblies in thin films (polymer brushes, multilayered films made of different polymers, hybrid systems that combine polymers and particles, thin films of polymer networks, and membranes that are thin films with channels/pores), and nanoparticles (micelles, nanogels, capsules and vesicles, core-shell particles, hybrid particle-in-particle structures, and their assemblies in solutions and at interfaces in emulsions and foams).

poly(*N*-isopropylacrylamide) (PNIPAAm) brushes that possess a lower critical solution temperature undergo a phase transition owing to changes in the solvent quality and temperature¹⁵. Polyelectrolyte brushes respond with large conformational changes to alternating ionic strength and pH¹⁹, whereas some zwitterionic brushes¹⁷ possess an upper critical solution temperature and change their wetting behaviour with temperature (Fig. 2d). These changes are reversible, and the material can sustain several transitions backwards and forwards.

The responsive behaviour of block copolymer brushes (Fig. 2b) is based on the phase segregation of different blocks, specifically when solvent affinities of each of the blocks are significantly different²⁰. The combination of different polymeric blocks in the responsive thin film results in a broadening of the switching range of properties, so that the surface property of the film changes from the property of one polymer to the property of the second polymer, or is locked in some intermediate state. A triblock poly(styrene-block-2-vinylpyridine-block-ethylene oxide) (PS-*b*-P2VP-*b*-PEO) copolymer brush is a representative example of a material in which external stimuli are used to tune the balance among electrostatic, steric and hydrophobic forces by exposing one or two polymers of these three constituent blocks to the thin-film boundary. This behaviour of the block copolymer brushes was used to tune interactions between the brush-decorated materials. For

example, the triblock-copolymer-coated pH-responsive colloids demonstrated switchable aggregation–dissociation of the particle assemblies (Fig. 2e)¹⁴.

In mixed polymer brushes (Fig. 2c), at least two chemically different polymers are grafted to the same substrate. Phase segregation causes the switching of the spatial distribution of the functional groups that are presented by the brush exterior so that the materials' properties are switched between the properties of two constituent polymers, similar to block copolymer brushes. Switching of surface composition and related physical properties in mixed brushes is a basic mechanism for dynamic changes of interactions between materials modified with the mixed brushes and their environment, including liquids and particulates. For example, a mixed polymer brush prepared from polystyrene and P2VP macromolecules changed the surface composition and wetting behaviour after treatment in different solvents¹³. The contact-angle change was found to be strongly amplified on a rough surface where the wetting properties switched from complete wetting to ultrahydrophobic behaviour⁷. It was shown that a mixed brush made of polystyrene and poly(methylmethacrylate) can induce the local motion (in the range of a few nanometres) of adsorbed nanometre-scale objects through solvent-induced topographical variations of the brush surface (Fig. 2f)¹⁸. A poly(ethyleneimine)–poly(dimethylsiloxane) mixed brush switched spontaneously from the hydrophilic state in

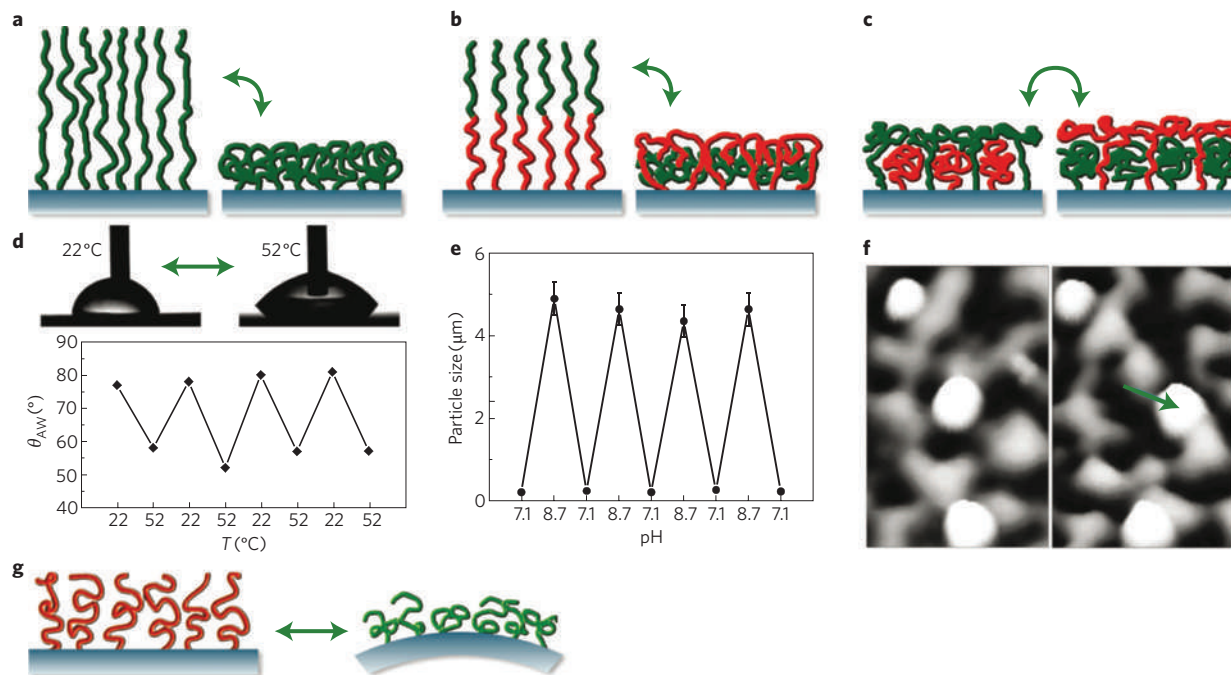


Figure 2 | Cartoons and photographs illustrating various architectures and responsive behaviour of polymers. **a**, Single-component homopolymer brushes. **b**, Block copolymer brushes. **c**, Mixed brushes. **d**, Change of the wetting characteristics of zwitterionic 2-(methacryloyloxy)ethyl dimethyl(3-sulphopropyl) ammonium hydroxide brushes after increasing the temperature from 22 °C to 52 °C, where θ_{AW} is the advancing water contact angle. **e**, Effective diameter of the silica particles and their aggregates covered with triblock PS-*b*-P2VP-*b*-PEO copolymer brush as a function of pH. The error bars represent the standard deviation of the experimental data (ref. 14). **f**, Atomic force microscopy (AFM) images acquired from the same area on the polystyrene-poly(methylmethacrylate) mixed brush covered with silica nanoparticles after a cycle of topographical variation of the thin film in different solvents. The position of three silica spheres relative to the underlying patterns of the brush can be pursued over cycles. The green arrow indicates the displaced silica particle. **g**, Deflection of cantilever versus time. Bias applied at the same time. With the cantilever at negative bias, the charges on the chain are drawn towards the cantilever, leading to large surface stresses and strong bending. At opposite bias, the counterions move towards the surface, resulting in smaller stresses but bending in the same direction. Figures reproduced with permission: **d,f**, © 2006 Wiley; **e**, © 2007 Wiley.

water to the hydrophobic one in air²¹. This adaptive behaviour of mixed brushes was used to develop materials with poor adhesion in a changeable environment. The surface coatings that were fabricated from mixed PEO-poly(dimethylsiloxane) brushes²² or from fluorinated nanoparticles and PEO brushes²³ were adaptive to liquid and vapour environments so that the surfaces were spontaneously transformed to non-sticky states in air and in water. This behaviour was observed on several cycles of exposure of the samples to air and aqueous solutions. If polymer brushes are grafted to a flexible substrate, the osmotic pressure in the brush may cause a deformation or bending of the substrate (Fig. 2g).

Nanostructured thin network films (that is, gel films, which are in many cases hydrogel films prepared from water-soluble polymers) are materials in which surface confinement brings a range of opportunities for engineering stimuli-responsive properties. An important attribute of gel thin films is their fast kinetics of swelling and shrinking compared with bulk gels. According to Tanaka and Fillmore's model²⁴, which shows the characteristic time of the swelling transition to be directly proportional to the square of the linear size of the gel, the response times are less than 1 s for gel films that are thinner than 10 μm . The swelling response of these films is highly anisotropic, because the attachment of the network to a surface prohibits in-plane swelling. Thus, the volumetric expansion of the network occurs exclusively in the direction perpendicular to the substrate plane²⁵.

Crowe-Willoughby and Genzer reported^{26,27} on the formation of polymeric materials with fast and tunable response times (that is, a few seconds) by chemically grafting poly(vinylmethylsiloxane) (PVMS) networks with alkanethiols bearing hydrophilic end groups ($-\text{COOH}$ or $-\text{OH}$). The rapid response (measured by the transition

from a hydrophobic state with a 110° contact angle in water to a hydrophilic one with a 55° contact angle) was facilitated by the liquid nature of the PVMS backbone, and it was found to decrease as the length of the methylene spacer ($-(\text{CH}_2)_n-$) in the alkanethiol pendant group decreased (Fig. 3a-c). For $n = 2$ and $n = 6$, the surface reconstructed almost instantaneously, whereas specimens with $n = 11$ resisted reconstruction because of strong van der Waals forces that led to the formation of semicrystalline regions.

Another important attribute can be found for porous thin gel films. It is well known that the swelling of porous bulk gels results in an increase in pore size. In contrast, surface-attached porous gel films demonstrate the opposite behaviour owing to the surface constraints²⁸. Switching between open and closed pores in thin gel films on shrinking and swelling, respectively, provides a unique opportunity for the regulation of transport through the film in a very broad diffusivity range from the level in solution down to a level in solids²⁹.

Thin responsive (hydro)-gel films can be used as freestanding films or on various supports (adhered or covalently grafted). These films can accommodate various chemicals, biomolecules and nanoparticles²⁹. In Fig. 3d,e, a porous P2VP thin gel film on the solid substrate shows pH-dependent porosity. The P2VP film is also responsive to cholesterol molecules (Fig. 3g,h). This response is used to tune the permeability of electrochemically active ions across a gel film that is placed on the surface of an electrode (Fig. 3i). The pH-dependent swelling of the P2VP film, which is loaded with gold nanoparticles, is used to tune the colour of the composite film with changes in plasmon coupling between gold nanoparticles (Fig. 3f)³⁰.

Electrostatic layer-by-layer (LbL) assembly has been introduced as a universal method for the facile fabrication of nanostructured,

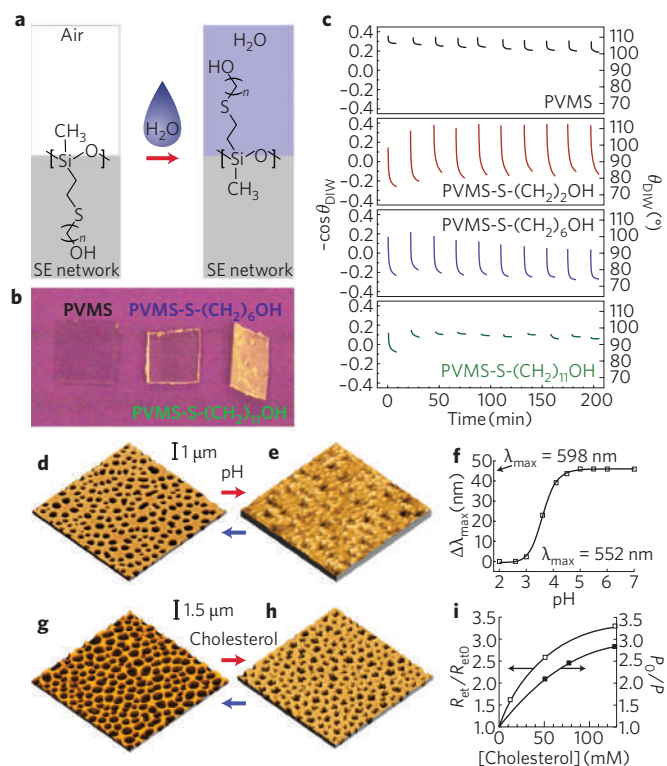


Figure 3 | Responsive behaviour of functional polymeric networks.

a, Schematic illustrating the molecular orientation of PVMS-S-(CH₂)_nOH at the air/sample and water/sample interfaces in the network samples. **b**, Photographs of PVMS, PVMS-S-(CH₂)₆OH and PVMS-S-(CH₂)₁₁OH specimens. The opaqueness of PVMS-S-(CH₂)₁₁OH is indicative of the presence of crystallites. **c**, Time dependence of the deionized water contact angles (θ_{DIW}) for PVMS-S-(CH₂)_nOH surfaces measured by dynamic contact angle set-up. The error for θ_{DIW} is $\pm 1.5^\circ$. **d, e**, AFM topography images ($7.5 \times 7.5 \mu\text{m}^2$) of a P2VP network thin film with pH-tunable porosity at pH 5.5 (**d**) and pH 2 (**e**). **f**, Shifts of the absorption maximum ($\Delta\lambda_{\text{max}}$) acquired from ultraviolet-visible spectra of a P2VP gel-gold nanoparticle composite film prepared on gold islands as a function of pH. **g, h**, AFM topography images ($10 \times 10 \mu\text{m}^2$) of a P2VP network film after washing in a chloroform solution with no cholesterol (**g**) and 0.13 M cholesterol (**h**). **i**, Normalized values of the electron-transfer resistance (open squares, derived from the Faradaic impedance spectra) and the film porosity (solid squares, derived from AFM measurements) shown as functions of the cholesterol concentration: R_{ct} and $R_{\text{ct}0}$ are the electron-transfer resistance values for the film with cholesterol and without cholesterol, respectively; P and P_0 are the porosities of the film with and without cholesterol, respectively. Figures reproduced with permission: **b-i**, © 2009 Wiley.

organized, multilayered, organic and hybrid thin films (Fig. 4a–c)^{31,32}. In the fabrication of LbL interfacial assemblies, Coulombic interactions, ion pairing, hydrogen bonding, and polar and hydrophobic interactions are exploited to facilitate alternative deposition of complementary species, including polyelectrolytes, nanoparticles, colloids and biomacromolecules, which form functionalized conformation nanostructured interfaces³³.

The mechanism of response of LbL assemblies was analysed by Rubner and co-workers³⁴, who attributed the dramatic variation in the degree of swelling (up to 400%) to changes in the degree of ionization of the weak polyelectrolytes (that is, poly(allylamine hydrochloride), PAH) where surface constraints affect the local environment of the ionizable groups. A sharp swelling and deswelling transition detected for LbL films at pH > 8.5 manifested itself in reversible pH-controlled variations of swelling percentage,

surface roughness and refractive index (Fig. 4a). The PAH swelling was associated with the variation in ionization of its free amine groups, and a hysteresis loop was related to the chain dynamics within swollen LbL films.

Recent studies exploited stimuli other than pH to alter the conformation and organization of the constituents of LbL films, including a response triggered by lower critical solution temperature at physiologically relevant temperatures (25–35 °C) by incorporating PNIPAAm interlayers³⁵; magnetically responsive free-standing LbL structures with incorporated iron oxide magnetic nanocrystals³⁶; or mechanically tunable elastic LbL films with a nanoporous interlayer acting as open–closed nanovalves when stretched and released from external mechanical stresses³⁷.

The architectures of the stimuli-responsive surfaces and mechanisms of their dynamic changes analysed in this section were successfully applied for the development of a range of stimuli-responsive materials and applications that are discussed below.

Smart and self-healing coatings. Reconstructable polymer surfaces form a toolbox for the rapidly developing field of smart coatings³⁸. The structure of the coatings can be programmed in the formulation. After deposition, external stimuli affect the phase separation of the ingredients to self-assemble into a coating with programmed properties. For example, colloidal particles prepared by the emulsion copolymerization of acrylate and fluorinated acrylate monomers can form stratified film morphologies, where the fluorinated phase can be driven to the film/air or film/substrate interfaces. As a consequence, static and kinetic coefficients of friction can be controlled at the film/air interface, resulting in superhydrophobic surfaces³⁹. In another example of programmed behaviour, colloidal particles are stabilized in an acidic aqueous solution by grafted PS-*b*-P2VP-*b*-PEO triblock copolymers. Casting of the particle suspension at higher pH results in a film consisting of particle aggregates, and, hence, a textured coating. The coating becomes superhydrophobic when heated to above the glass-transition temperature of polystyrene blocks, because these blocks migrate to the top-most layer of the coating⁴⁰.

Coatings with self-healing capabilities fall in the category of smart coatings with a programmed structure and response⁴¹. A multilayered LbL system made up of polyelectrolytes and a corrosion inhibitor could heal the corrosive area on a metal substrate and release the inhibitor during a corrosion attack. The origin of such self-healing behaviour lies in the breaking and re-establishing of polyelectrolyte complexes in response to changes in a corrosive environment (that is, high ionic strength)⁴².

Biointerfaces and bioseparation. The responsive properties of reconstructable thin polymer films are relevant to many biotechnological and biomedical applications^{5,43,44}, because these films can undergo dynamic changes in accord with changes in living systems.

Several key aspects have attracted interest in stimuli-responsive polymeric biointerfaces. First, the possibility of tuning and switching adhesion between stimuli-responsive materials and proteins and cells has been explored for the control of cell⁴⁵ and protein^{46,47} adhesion, and used for tissue engineering and bioseparation. Second, the possibility of exposing and masking functional moieties at the biointerface is very important for the presentation of regulatory signals and concomitant modulation of biomolecule activity⁴⁸ for cell research and bioengineering. Recently, PNIPAAm and its copolymers have been functionalized with recognition moieties (for example, synthetic peptides) that interact with cell components. Ebara *et al.*⁴⁹ used stimulus-responsive PNIPAAm-based copolymers to expose or mask arginine–glycine–aspartic acid (RGD) recognition sequences for cell binding.

Third, the possibility of dynamic control of the permeation of chemicals through nanoporous membranes^{10,28–30,50} or the

interaction of biomolecules and ions with responsive surfaces^{47,51,52} offers a unique opportunity for bioseparation^{52,53}. Surface-grafted stimuli-responsive polymers provide an exciting means for controlling drug permeation through nano- and microporous membranes. Systematic work that explores the complex interrelationship among pore size, polymer molecular weight, grafting density and drug-permeation flux has only recently begun^{50,52,53}.

Micro- and nanoactuation. Light-, pH- and temperature-responsive thin polymer films have been used for micro- and nanoactuation. Actuation by means of responsive polymer brushes originates from variable stretching of grafted macromolecules as a result of the strong steric repulsive interactions between neighbouring chains. In charged polyelectrolyte brushes, osmotic and Coulombic forces often lead to extra repulsive interactions and increase the level of reversible chain stretching. The forces that affect the conformations of tethered polymers on solid substrates can be harnessed for actuation by growing brushes on flexible substrates. The brush can transduce these forces into lateral surface stresses⁵⁴ that cause the substrate to bend. As a result, bending can be modulated by charge screening with the use of solutions of varying ionic strength or pH^{55,56}.

It was recently demonstrated that applied electric fields lead to the actuation (1–5 Hz) of cantilevers through the switching of surface stresses in polyelectrolyte brush films (Fig. 2g)⁵⁷. The presence of triggered reversible contraction and expansion of polymer brushes offers a design rule for nanoscale actuation that does not rely on chemical fuels such as acids and bases.

So far a variety of actuation mechanisms (and therefore sensing mechanisms) have been realized for flexible structures (mostly silicon microbeams coated with organic films) based on the swelling and de-swelling, wetting and de-wetting, or adsorption and desorption of organic surface layers⁵⁸. Recent work on nanopatterned thermoresponsive brushes provides more insight into the challenges that lie ahead. In nanopatterned brushes, polymer chains are in a slightly different chemical environment; some are in the middle of a 'sea' of polymer chains whereas others lie at the edge and will be required to wet and de-wet from the surrounding surface. As a result, all chains show subtle differences in the degree of chain stretching and thermoresponsive properties, thus leading to an overall broadening of the collapse temperature that is often extremely narrow in the bulk^{59,60}. The main disadvantage of the brush-based actuators is their relatively slow response compared with polymer-gel-based systems^{61,62}, which probably results from a difference in chain packing. The dense packing leads concurrently to unique properties that are found only in polymer brushes and that could be ideal for sensor applications. For example, large end groups in dense brushes will be 'expelled' from the brushes; any (reversible) decrease in the size of these head groups will lead to the rapid contraction of the associated polymer chains into the brush layer⁶³.

Sensors. That stimuli-responsive polymer systems facilitate efficient transduction mechanisms makes them suitable for use in sensor applications. For example, Tokareva *et al.*⁶⁴ demonstrated the tuning of the plasmon-resonance coupling between gold nanoparticles and a gold substrate mediated by a 20-nm-thick swellable P2VP brush layer. The film can be used as a highly sensitive pH-responsive nanosensor with short response times. The authors demonstrated a large (50 nm) shift in the plasmon-resonance position as a result of changing pH values (within pH = 3.8 ± 0.5) caused by shrinking of the brush thickness from 22 to 7 nm. Internal stresses caused by conformational transformations within brush layers were used to design pH-sensitive microsensors by grafting PNIPAAm onto microcantilevers¹⁵. This design provided a high level of sensitivity, reaching 121 nm of deflection per pH unit. The use of poly-L-lysine-PEO-biotin brushes grafted inside a microchannel carved within a microcantilever allowed for the subfemtogram detection

of the selective binding of γ -IgG (immunoglobulin G) in fluid, representing a dramatic improvement of sensitivity over a conventional quartz microbalance⁶⁵.

Different LbL films with embedded biomolecules and nanoparticles have been exploited as soft organized matrices for uploading nanoparticles to fabricate pH-responsive and biosensing nanomaterials based on the surface plasmon resonance (SPR) phenomena⁹. As well as conventional metal nanoparticles, which show SPR peaks in the range of 520–540 nm (refs 64,66), recent studies expanded this approach towards sensors that contain gold nanorods⁶⁷. Specifically, gold nanorods were embedded in crosslinked poly(methacrylic acid) (PMAA)-PAH and PMAA-poly(*N*-vinylpyrrolidone) LbL films to act as pH-responsive plasmonic sensors (Fig. 5). Swelling and de-swelling of these gels at pH 8 and pH 5, respectively, resulted in reversible and large shifts of a strong, easily detectable longitudinal plasmon resonance located in the near-infrared region (\approx 700 nm) owing to variable side-by-side nanorod interactions.

Colorimetric or electromechanical detection methods that are used for the reversible and dramatic reorganization of LbL coatings, and that are typically triggered by pH or ionic strength, are achieved by the incorporation of inorganic nanoparticles with the characteristic optical signature and the conformal nature of LbL films. For example, Kotov *et al.*⁶⁸ demonstrated reversible loading and unloading of quantum dots in highly hydrated LbL films from poly(diallyldimethylammonium chloride) and polyacrylic acid (PAA). These structural variations were accompanied by corresponding changes in fluorescence. Changes in photoluminescence and plasmon resonances in the visible range have been observed for conventional PAH-poly(styrene sulphonate) (PSS) LbL films and LbL films that contain amine-terminated dendrimers^{69,70}. A strong and easily detectable optical response was achieved by placing LbL films that contained either dyes or gold nanoparticles on gold substrates to exploit either a quenching mechanism or coupling plasmon resonances.

The responsive behaviour of thin hydrogel films has attracted great interest for a range of applications in sensors, including chemical gating^{28–30,51}, microgravimetric, micromechanical or optical transduction of chemical signals^{71,72}. Responsive 3D 2-hydroxyethylmethacrylate hydrogel and PNIPAAm colloidal crystals showed rapidly tunable photonic bandgaps in infrared regions^{73,74}; free-standing flexible PAH-PSS films acted as pressure and acoustic sensors⁷⁵; and PNIPAAm-PAA microlenses with tunable focal lengths allowed for autonomous focusing under external pressure⁷⁶. In the case of the PNIPAAm-PAA microlenses, it has been suggested that the tuning of the focal length is controlled by variations in the refractive index of the swollen or shrunken material caused by protonation or deprotonation of the acidic groups, temperature, or physical crosslinking or decrosslinking events⁷⁷ (such as binding or release of antibodies). The tunable microlens arrays can be integrated into microfluidic and lab-on-a-chip technologies for biosensing and medical diagnostics. Recently, a reversible switching of pillar arrays embedded in humidity sensitive gel films that can be used as tunable microfluidic sensors has been demonstrated⁷⁸; and an intriguing model of mechanochemical transducing gels has also been constructed⁷⁹. The computer simulations in these studies suggested that adaptive gel materials can sense local stresses by generating chemical waves and therefore potentially could be used as touch-sensitive sensors.

From two to three dimensions: responsive particles

Stimuli-responsive colloidal particles represent a rapidly developing class of stimuli-responsive materials that find applications in the stabilization, destabilization and inversion of colloidal dispersions (emulsions, foams and suspensions), in catalysis, sensors and drug-delivery capsules (Fig. 4b,c).

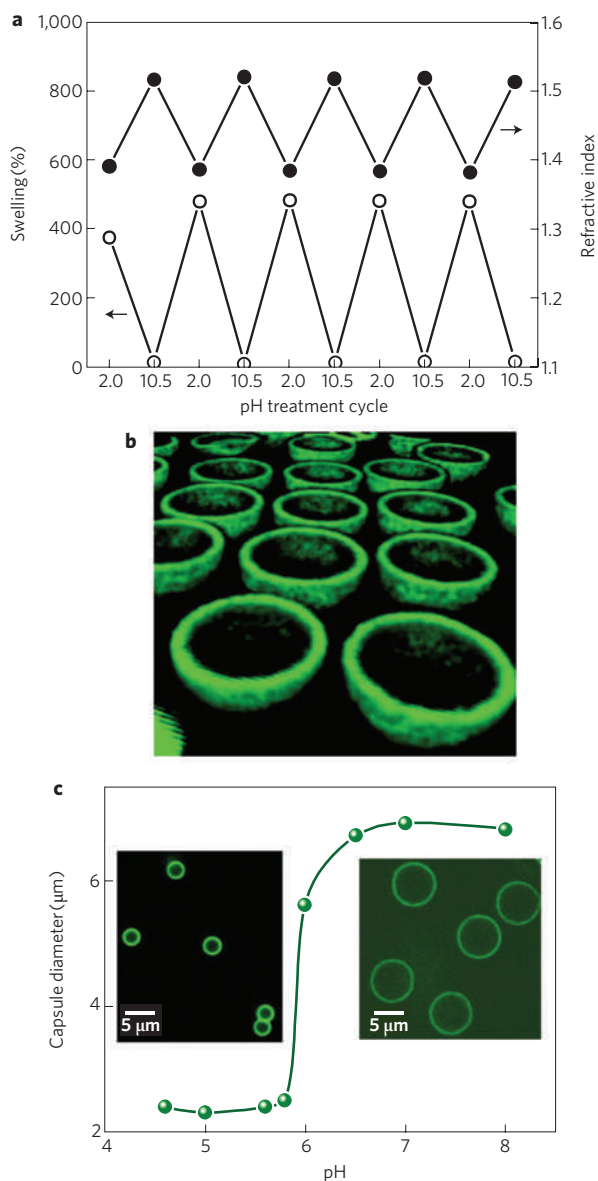


Figure 4 | Responsive properties of polyelectrolyte thin films and capsules prepared by the LbL method. **a**, Swelling and refractive-index variation during alternating pH treatment of LbL PSS–PAH films. **b**, 3D reconstruction of the confocal images of the 3- μm LbL PMAA microcapsules. **c**, pH-dependence of the diameter of the crosslinked PMAA microcapsules. Figures reproduced with permission: **a**, © 2005 ACS; **b**, © 2008 ACS; **c**, © 2006 ACS.

Configurational design. The configurational design of responsive nanoparticles can be typically represented by a core–shell architecture formed through self-assembly of amphiphilic copolymers (polymer micelles or vesicles) or by means of surface modification of various particles (inorganic or polymeric) with functional polymers. The core-forming polymer (in micro- and nanogels), shell-forming polymer, or both core and shell polymers can show stimuli-responsive behaviour (Fig. 6a–d). External stimuli are used to stimulate the self-assembled structures and may induce their reversible or irreversible disintegration, aggregation, swelling and adsorption. The toolbox of responsive colloids includes functional polymers, copolymers and inorganic nanoparticles.

Block copolymers form various types of self-assembled structure, from micelles to continuous bilayers, depending on the solvent selectivity of the different blocks^{80,81}. The application of external stimuli in these systems may lead to a change in the aggregate size

and/or to changes in the aggregate architecture and structure; that is, transformation from a spherical micelle to a polymersome in an aqueous medium, or the interchange between the blocks in the core and the corona. Polyelectrolyte micelles are obtained from stoichiometrically mixed, oppositely charged macro-ions, provided that one of the ingredients is a charge-neutral hydrophilic diblock copolymer. The purpose of this neutral block is to prevent the formation of a macroscopic polyelectrolyte complex by protecting the core (which consists of the complex) with a neutral and hydrophilic corona (Fig. 6a). As a variant, one can use charged inorganic nanoparticles⁸² and self-assembled macro-ions as the second ingredient⁸³ or two diblock copolymers with two different neutral blocks. In the case of two different neutral blocks, a phase-separated corona can form fully equilibrated, yet symmetry broken, dumbbell-like particles (that is, Janus micelles)⁸⁴.

Polymer vesicles (polymersomes, in which the central aqueous compartment is enclosed by an amphiphilic copolymer membrane) are another example of self-assembled stimuli-responsive polymer structures. The copolymer membrane regulates transport of molecules between the inside and outside of the vesicle; the permeability is tunable and degradation of the membrane can be triggered by external stimuli⁸⁵. Incorporation of pH-responsive domains, which renders the vesicle capable of regulating the transport of hydrophilic molecules across the membrane, results in a shell that resembles the transmembrane channels of living cells⁸⁶.

Nanoparticles that possess an internal network structure — that is, they have properties of hydrogels — are called nanogels (Fig. 6b)⁸⁷. A simple and effective approach to heat-sensitive nanogels involves PNIPAAm–polysaccharide (graft) copolymers, which are soluble in cold water and self-assemble into nanogels as a result of the heat-triggered collapse of the PNIPAAm chains⁸⁸. Such nanogels disintegrate on cooling. Nanogels can also be designed to be reversibly responsive to two different stimuli, for example, temperature- and redox-sensitive nanoparticles⁸⁹.

Stimuli-response macromolecules have been incorporated into the outer shell of hybrid colloidal core–shell particles (Fig. 6c,d). Often, an inorganic material with specific optical or magnetic properties is chosen for the core. The properties of the shell can be tuned by physico-chemical means, so that the tendency of particles to aggregate and their affinity for liquid interfaces can be reversibly manipulated. The result is the reversible regulation of the microscopic and macroscopic properties of colloidal dispersions (for example, sols, suspensions, emulsions and foams) under the action of suitable external stimuli. For example, a pH-responsive polymer shell grafted to the surface of silica nanoparticles controls the nanoparticles' reversible aggregation and deaggregation, and can be coupled with pH changes owing to a complex combination of biocatalytic reactions (Fig. 6d)⁹⁰.

Layer-by-layer assembly has been applied successfully for a template fabrication of responsive capsules by coating micrometre- and submicrometre-sized particles (Fig. 4b)^{91,92}. After the core has been coated with an LbL shell, the colloidal core can be dissolved, therefore leaving hollow capsules. In general, these microcapsules show a responsiveness that is similar to that of LbL films (Fig. 4c)^{93,94}. The LbL microcapsules made of composite polyelectrolytes and nanoparticle shells can be manipulated by remote physical stimuli (for example, magnetic field and light).

Stimuli-responsive particles could find use in numerous applications in the chemical, coatings, cosmetic, detergent and food industries, as well as drug delivery and diagnostics where the stimuli-triggered formation, disintegration, or inversion on demand of the particles and their dispersions could be used for the development of new technologies and products.

Stimuli-triggered stabilization of colloidal dispersions. Amphiphilic responsive colloidal particles can be introduced into

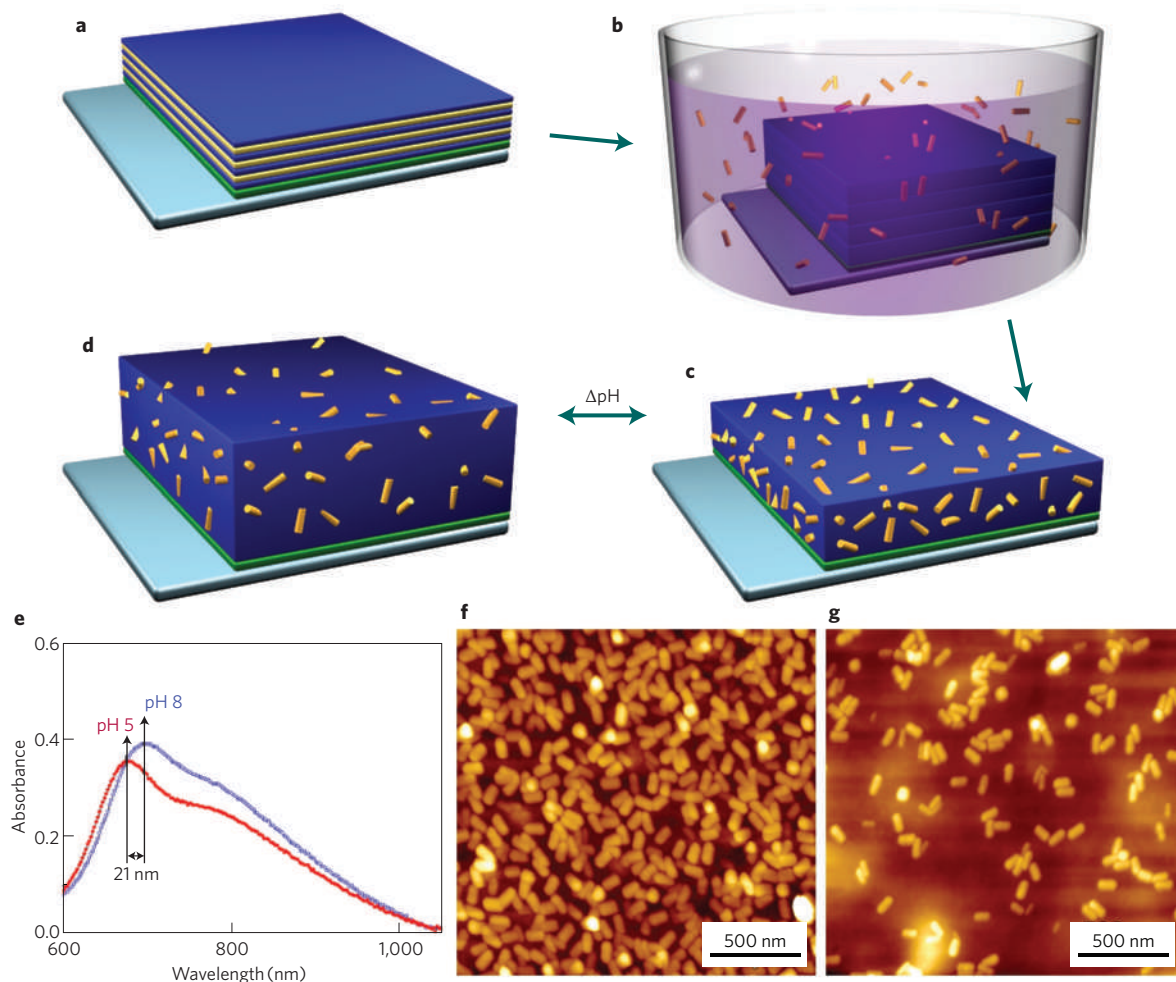


Figure 5 | Hydrogen-sensitive LbL hydrogels. **a**, LbL assembly of PMAA/poly(*N*-vinylpyrrolidone) films. **b**, Swelling crosslinked hydrogel in a solution of gold nanoparticles. **c,d**, Swelling of nanorod-LbL film can be controlled by pH resulting in a shift in longitudinal SPR peak. **e**, Shift in plasmon resonance of gold nanorods caused by gel swelling. **f,g**, AFM images show gold nanorods embedded into a LbL gel. Figures reproduced with permission: **e-g**, © 2008 ACS.

the interface between two immiscible fluids (that is, liquid/liquid or liquid/gas), where the particles are strongly pinned owing to their large surface areas. They can then stabilize emulsions and foams (Pickering dispersions), primarily as a result of the formation of a mechanical barrier that prevents the coalescence of the dispersed phase and that reduces the bending rigidity of the interface. More hydrophobic particles preferentially stabilize water-in-oil emulsions (because asymmetric positioning in the interface imposes a tendency to curve towards the least preferred phase), and vice versa. Hence, a key parameter is the preference of the particles for either phase. The particles will expose a larger fraction of their surface to the liquid phase that has a higher affinity to the particle surface; this phenomenon can be used to produce various effects. For example, detaching particles entirely from the interface is possible in the presence of a sufficiently strong shift (induced by external stimuli such as a pH change) in the interaction balance towards a preferential liquid phase (Fig. 6c). Particles are then pulled off the interface into the selective phase^{14,95}, and the emulsions ‘break’. Milder shifts lead to the inversion of emulsions and foams (that is, from air-in-water foam to water-in-air powder)^{96,97}.

Tunable catalysis. The possibility of exposing or hiding functional groups or nanoparticles in the reconstructable surfaces has opened new directions in chemical and biochemical catalysis. For example, Ballauff *et al.*^{98,99} described a switchable catalyst that was made by synthesizing 10-nm metal nanoparticles inside a thermoresponsive

polymer shell that had been grafted to the surface of a much larger colloidal particle. Temperature-dependent swelling and shrinking of the shell were used to alternatively expose and hide the silver nanoparticles on the surface of the colloids, thereby modulating the catalytic activity of the composite particle. Conjugation of stimuli-responsive polymeric systems with catalytic nanoparticles and enzymes could thus create new opportunities for bio- and chemical technologies.

Drug delivery. Recently, stimuli-responsive nanoparticles and nanocapsules have attracted great interest because of the broad opportunities for *in vivo* applications. Such nanosized capsules could store and protect various drugs, and release them inside cells after the capsule has been internalized. A smart drug-delivery polymeric system should undergo a complex chain of responses to survive *in vivo*, deliver the cargo, release the drug into the target cells, and match the desired kinetics of the release. Among the various approaches used to enhance the efficacy of chemotherapy is the use of carrier systems that release a drug in response to stimuli, such as changes in pH, glutathione concentration, or the presence of specific enzymes that are selectively encountered in relevant cell organelles.

Hollow LbL capsules can be refilled with various molecules for drug delivery. Drug release can be activated on demand by local changes in pH or by remote physical stimuli. For example, Skirtach *et al.*¹⁰⁰ demonstrated the selective addressing of intracellular LbL microcapsules with laser light. Kreft *et al.*¹⁰¹ demonstrated pH

monitoring and LbL microcapsule tracking inside cells through the encapsulation of pH-sensitive dyes. One of the limitations of the capsule applications is the size of the capsule. Although most reports consider capsules in the micrometre range, only a few attempts have been made to fabricate LbL capsules smaller than 200 nm in diameter. It is prudent to stress that the optimal size for an efficient delivery to cells and internalization within them is considered to be in the range 25–100 nm.

Micelle-like nanoparticles can easily approach the submicrometre scale. Several types of such micelle-like nanoparticle and vesicle have been prepared based on block copolymers and polyelectrolyte complexes. For example, linear-dendritic block copolymers composed of a linear PEO block and either a polylysine or polyester dendron were used for the fabrication of pH-responsive micelles for drug delivery¹⁰². It was shown that an encapsulated agent can be stored in prepared micelles at pH 7.4 and released at pH 5 by means of gradual disintegration of micelles into unimers.

In polyelectrolyte micelles, electrostatic forces keep these particle assemblies together. It is obvious that they respond to added salt¹⁰³. If the core is made of weak polyelectrolytes the integrity of

the particles is pH-dependent, because the balance between the positive and negative charges is affected. Such particles, loaded with drugs and enzymes, become unstable and release the drugs on changes in pH¹⁰⁴.

Stimuli-responsive nanogels represent another type of promising material for drug delivery. Nagasaki's team prepared nanogels from a crosslinked, pH-sensitive polyamine core, surrounded by PEO chains that were conjugated to ligands recognized by cell-specific receptors¹⁰⁵. These nanogels were internalized by cells through receptor-mediated endocytic pathways. In the acidic endosome, the nanoparticles swelled and released drugs sequestered in the particle core. Furthermore, a virus-mimetic nanogel was developed by Bae and colleagues¹⁰⁶. These nanogels possess the trademark property of viruses to migrate from one cell to another, leaving part of their cargo behind. The virus-mimetic nanogels consist of a drug-loaded copolymeric core surrounded by a PEO-bovine serum albumin double shell that is decorated with folate groups able to bind to specific cell receptors. Internalized virus-mimetic nanogels enter the endosomes, where the nanogels experience a pH-triggered volume expansion that is accompanied by the release of the drug. However, the swollen nanogels disrupt the endosomal membranes and escape from the endosome. The nanogels then encounter a less acidic pH, shrink back to their initial size, and migrate to another cell, just as a virus does.

The discussed examples demonstrate the essential progress in the area of smart drug-delivery systems. Capsules and vesicles show much higher drug-loading capacity than micelles and nanogels. Capsules and nanogels are much more stable than micelles and vesicles. The kinetics of drug release can be adjusted across a very broad range by the conjugation of drugs with macromolecules and the regulation of the transport across the capsule wall. Stability (both mechanical and chemical) can be regulated by crosslinking of the polymers. Prolonged circulation *in vivo* has been accomplished by modification of the outer shell with PEO brushes, and target delivery could be solved through the incorporation of specific ligands on the shell. An ideal drug-delivery device could be foreseen as a 25–100 nm capsule decorated with the PEO brush and ligands (specific for target cells). The shell should be an impermeable film with stimuli-responsive pores for triggered gating of the drug release. The release dynamics should be regulated by the precise control of the open-pore dimensions and/or by conjugation of the drugs with macromolecules.

Challenges for modelling, simulation and theory

The structure of stimuli-responsive polymer systems is dictated by a subtle interplay among non-bonded interactions, the conformational entropy of the macromolecules, and frozen constraints resulting from irreversible grafting and network formation, or the geometry of the substrates. The description of these collective phenomena requires a coarse-grained approach. Scaling considerations and self-consistent field theory^{107–109} as well as particle-based simulations^{110,111} have been used in conjunction with coarse-grained models to investigate, *inter alia*, the properties of polymer brushes, polyelectrolyte layers and the phase separation in multi-component networks.

Although standard coarse-grained models¹¹² and systematic coarse-graining procedures^{113,114} are available for simple systems, the development of coarse-grained models of stimuli-responsive, multicomponent systems in aqueous solution is still in its infancy.

For practical applications, the kinetics of structural changes in the presence of external stimuli is most relevant. Although it is a prerequisite for designing systems with rapid switching times, it sometimes remains unclear if equilibrium can be attained on the pertinent experimental timescale. Thus, the kinetics may dictate the observed structure. The investigation of the temporal re-arrangements in response to external stimuli has just begun^{115,116}.

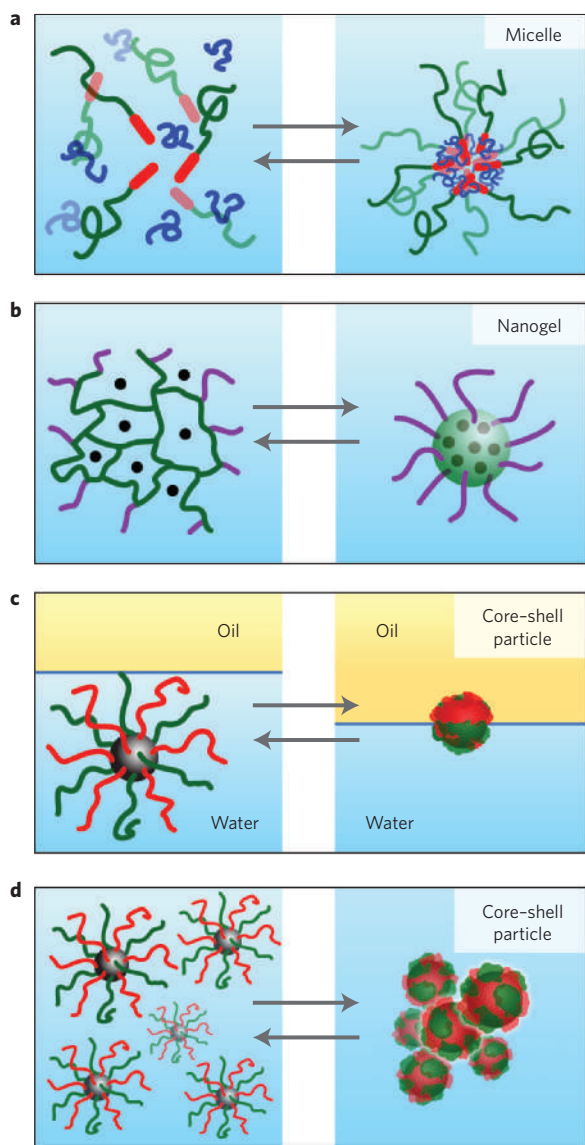


Figure 6 | Various configurational schematic designs of stimuli-responsive nanoparticles. **a–d**, Micelles (**a**), nanogels (**b**), and core-shell particles in suspensions (**c**) and at interfaces (**d**).

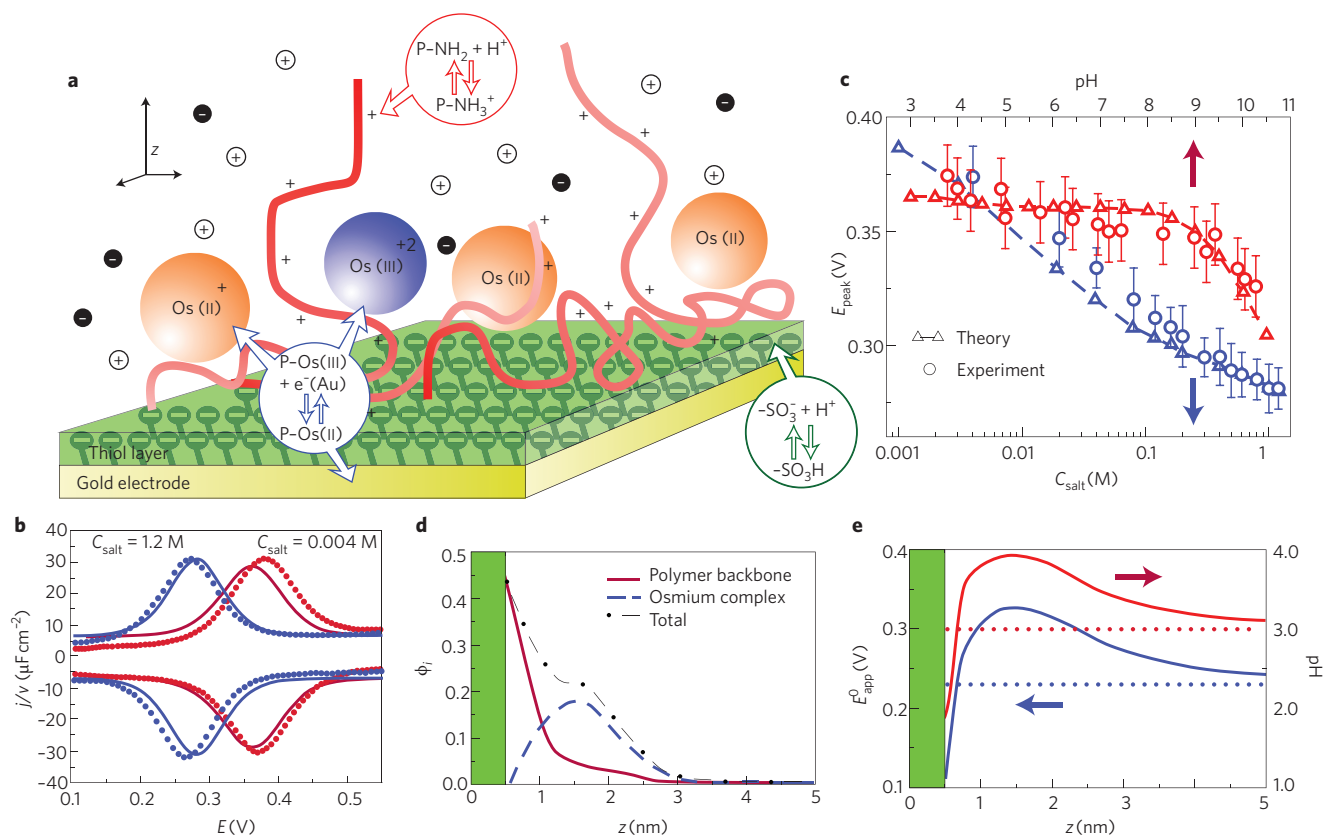


Figure 7 | A gold electrode modified with a mercaptopropyl sulphonate (MPS) self-assembled monolayer, with adsorbed redox polymer. **a**, Schematic representation, with the poly(allylamine) backbone of the redox polymer-osmium (PAH-Os) shown as red curves and the tethered pyridine-bipyridine Os complexes as orange or blue spheres according to their oxidation state. The allylamine units can be either in a positively charged protonated state (plus signs on the polymer-backbone lines) or in a neutral deprotonated state, which are related by an acid-base equilibrium. The sulphonate groups in MPS are in acid-base equilibrium with protons in solution and thus could be protonated or deprotonated. The polymer-modified electrode is immersed in an aqueous electrolyte solution containing salt ions, protons and hydroxyls in thermodynamic equilibrium with a bulk solution. The normal direction from the electrode is denoted by z and has its origin on the metal surface. **b**, Comparison of experimental (circles, $V = 0.025 \text{ V s}^{-1}$) with theoretical (solid lines) current density (j) divided by the scanning velocity (v) versus voltage (V) plots measured for a Au/MPS/PAH-Os electrode in solutions of different ionic strength and 1 mM HNO_3 (pH 3). **c**, Plots of experimental and theoretical peak potential position as a function of bulk salt concentration (lower axis, blue symbols) and bulk pH (upper axis, red symbols). The error bars represent the standard deviation of the experimental observations (ref. 123). **d**, Theoretical volume-fraction profiles for the polymer backbone (red full line), the redox sites (blue dashed line) and the whole redox polymer (black dot-dashed line) for $E = E^0_{\text{Os(III)/Os(II)}}$ concentration ($C_{\text{salt}} = 0.1 \text{ M}$) and pH = 3. The shaded region ($z < 0.5 \text{ nm}$) is occupied by the thiol layer. **e**, Distance-dependant formal Os(III)/Os(II) redox potential (blue line, left axis) and local pH (red line, right axis) as a function of the distance from the electrode calculated for the same experimental conditions as those described in **b**. The bulk values are shown by the dashed lines. Figure reproduced with permission: **d**, © 2008 ACS.

Molecular modelling of responsive polymer layers. One important aspect of responsive polymer layers is the coupling that exists between the conformational degrees of the chain molecules, the specific intra- and intermolecular interactions, and the possibility of reversibly regulating chemical reactions within the polymer layer. The basic idea is to look at each molecular species with as much molecular detail as possible while treating intermolecular interactions within a mean-field approximation. These approaches predict both thermodynamic and structural properties and can incorporate many of the different interactions^{117–119}, hydrogen bonding¹²⁰ and chemical reactions^{118,121–123} present in these systems. The inclusion of molecular-level detail of the polymers allows the structure of the layers to be described in great detail using density functional theory^{119,124}, self-consistent field theory^{118,121,125}, and single-chain (molecular) mean-field theory^{117,120,122}. The main differences among these approaches are in the level of detail with which the molecules are treated; in fact, they become equivalent within certain limits^{117,124}. These approaches have shown good predictive power, but they also have several limitations such as the lack of intermolecular correlations and the assumption that the systems are laterally homogeneous so

that surface domains^{109,126} cannot be treated. Also, the incorporation of electrostatic interactions within a mean-field approach can be problematic in some regimes¹²⁷.

An example of a highly complex responsive layer is a redox-polymer-modified electrode (Fig. 7a–e). This layer responds to changes in pH, solvent quality, solution ionic strength and applied electrode potential^{122,123}. Figure 7 shows the predictive power of theory as a function of pH and ionic strength for the reversible curves of current density divided by scanning velocity versus potential (Fig. 7b,c). Moreover, the theory explains the molecular organization within the film. The most important feature is that even within the 3 nm thickness of the film, the distribution of polymer segments and redox (osmium) sites (Fig. 7d), the local proton concentration and the apparent potential (Fig. 7e) are highly inhomogeneous. These very large local changes are important because they determine the true state of the film.

Particle-based simulations of large 3D assemblies. Computer simulations of particle-based models require substantial computational resources. To study the self-assembly and phase separation of

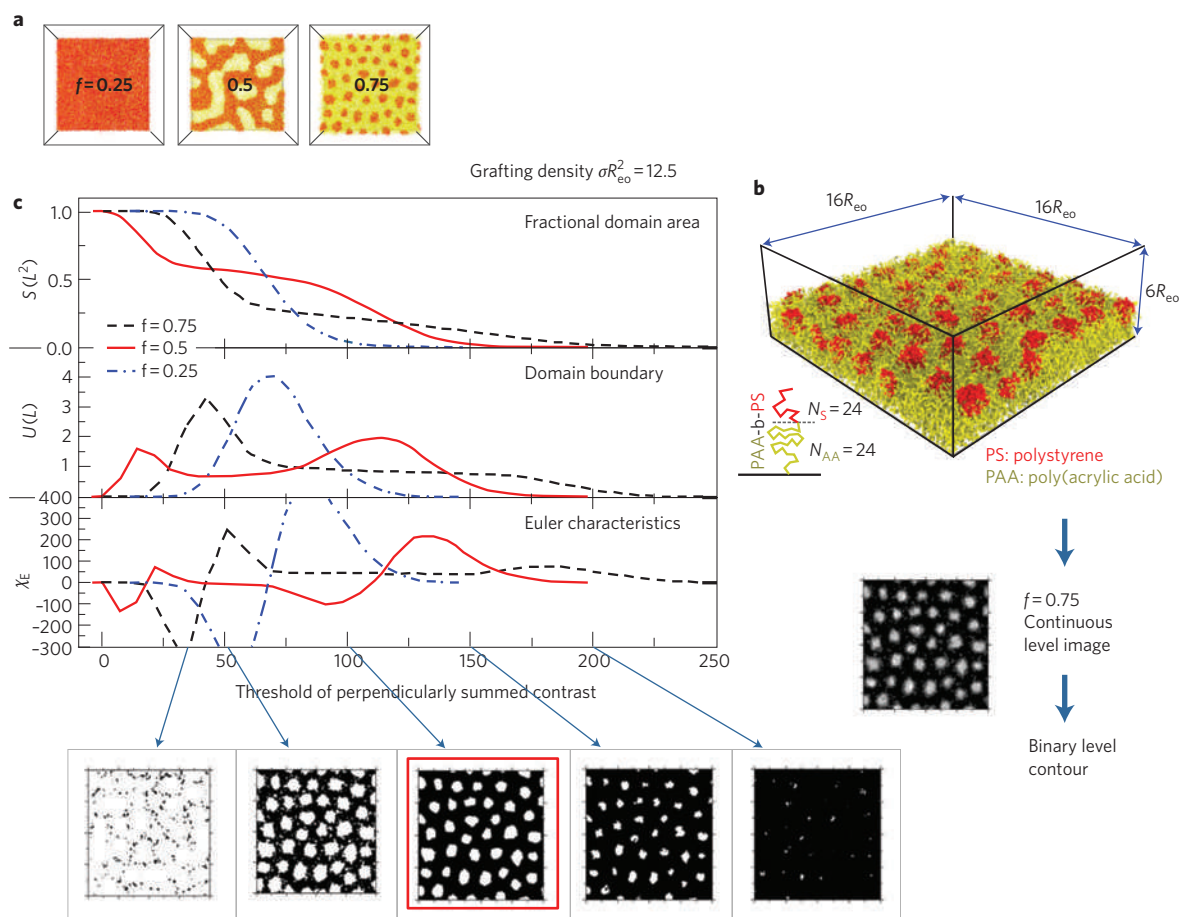


Figure 8 | Molecular structure of a diblock copolymer brush observed by single-chain-in-mean-field simulations showing lateral phase separation. The system mimics a PAA-polystyrene diblock copolymer brush in water at high pH value. **a**, Top view of morphologies for different values of molecular asymmetry (f). PAA is shown in yellow, whereas polystyrene is depicted in red. On increasing the fraction of the bottom block, PAA, we observe a gradual crossover from a continuous, collapsed polystyrene layer ($f = 0.25$), a perforated layer ($f = 0.5$) to spherical micelles ($f = 0.75$). **b**, Reduction from a 3D snapshot of a configuration with $f = 0.75$ (that is, diblock copolymers represented by $N_{AA} = 24$ coarse-grained PAA segments and $N_S = 8$ polystyrene segments), by means of a continuous 2D level image to a 2D binary contour with different threshold values, which is analysed by Minkowski measures. **c**, Minkowski measures characterizing the disordered morphology: fractional domain area, S , measured in units of the lateral system size, $L^2 = 256R_{eo}^2$ (R_{eo} being the polymer's end-to-end distance), length of the domain boundary (U) in units of L^2/R_{eo} , and Euler characteristics (χ_E). The Minkowski measures are analysed as a function of the threshold, Σ_ρ of the vertically averaged density (ρ) difference providing information about the type of morphology (ripple versus dimple/spherical micelles), the segregation and spatial extension of the domains. The plateau value of χ_E quantifies the number of domains in the dimple morphology (spherical micelles), whereas breaking up of the structures, signalled by large absolute values of χ_E indicates that they do not span the entire film thickness (σ is the grafting density). Figures reproduced with permission: **b,c**, © 2009 ACS.

large, 3D systems, coarse-grained models with soft potentials have been devised¹²⁸. In these models, the absence of excluded volume allows the beads, which represent the centre of mass of a few atoms, to overlap. Thus, systems with an experimentally large and invariant degree of polymerization and realistic fluctuations can be described. The soft interactions can be pair-wise (for example, dissipative particle-dynamics models¹²⁹) or they can take the form of a density functional model, which allows for a close connection with the molecular, mean-field approaches (described above) and which incorporates the rich thermodynamics of multicomponent systems¹³⁰. These models have been applied for the study of, for example, the strong amplification of quenched fluctuations in the grafting-point density by the structure formation in a mixed polymer brush. This effect causes the morphology to be correlated between different cycles of stimuli switching (that is, domain memory measure^{131,132}) and prevents the formation of long-range periodic order. Thus, the structure factor of lateral density and composition fluctuations does not distinguish clearly between different disordered morphologies. This absence of long-range order is also observed

in the phase-separated morphology of diblock copolymer brushes (Fig. 8), and Minkowski measures have been used to characterize the structures of these brushes¹²⁸.

Future directions

Responsive polymer systems can be used for a variety of applications, such as switching surfaces and adhesives, protective coatings that adapt to the environment, artificial muscles, sensors and drug delivery. Biochemistry, environmental sciences and biomedical sciences are just a few examples of important areas that will benefit greatly from further development of applications of stimulus-responsive polymeric materials. In fact, it is a challenge to develop complex systems that are responsive to biochemical signals or biomarkers typically present in a less than nanomolar concentration range. Such systems-within-systems need a complex, hierarchical organization of the responsive particles discussed here to accommodate various possible amplification mechanisms. A hierarchical organization (for example, hierarchical compartmentalization) will also be important for the development of systems where the functions of 'receiving'

the signal and 'responding' by changing the material's properties are separate because, in some cases, the changes affected by the stimuli may interfere with the desired changes in the material's properties. In living systems, nature broadly exploits the principle of partitioning; local dynamic changes take place in compartments that are separated by permselective membranes. This type of organization in stimuli-responsive materials will provide great opportunities with regard to a programmable, complex response of the materials.

Another challenge is to develop systems that can respond to several external stimuli in an intelligent way. Although several examples of such 'biocomputing' systems^{51,90,133,134} and surface-encoded assemblies of nanoclusters¹³⁵ have been reported recently, much more remains to be done before practical applications are viable.

One significant challenge that is inherent to almost all organic systems pertains to long-term stability (that is stability to temperature, ultraviolet light, solvent vapours and so on) and durability (that is, mechanical stability, abrasion and so on).

Responsive systems can be introduced into many products at a relatively low cost, because often only a very thin (nanometre-thick) coating is required. Providing added functionality with such a coating can enhance the value of a product significantly — for example, materials that are capable of repairing themselves in less than an hour can be used in many coatings applications ranging from decoration to biomedical industries¹³⁶. The concepts presented in this review will be beneficial for many new applications in the future because they will allow for the introduction of new aspects and possibilities in the field of conventional materials.

References

- Senaratne, W., Andruzzi, L. & Ober, C. K. Self-assembled monolayers and polymer brushes in biotechnology: Current applications and future perspectives. *Biomacromolecules* **6**, 2427–2448 (2005).
- Jhaveri, S. J. *et al.* Release of nerve growth factor from HEMA hydrogel-coated substrates and its effect on the differentiation of neural cells. *Biomacromolecules* **10**, 174–183 (2009).
- Hoffman, A. S. The origins and evolution of "controlled" drug delivery systems. *J. Control. Release* **132**, 153–163 (2008).
- Bayer, C. L. & Peppas, N. A. Advances in recognitive, conductive and responsive delivery systems. *J. Control. Release* **132**, 216–221 (2008).
- Mendes, P. M. Stimuli-responsive surfaces for bio-applications. *Chem. Soc. Rev.* **37**, 2512–2529 (2008).
- Luzinov, I., Minko, S. & Tsukruk, V. V. Responsive brush layers: from tailored gradients to reversibly assembled nanoparticles. *Soft Matter* **4**, 714–725 (2008).
- Motornov, M. *et al.* Reversible tuning of wetting behaviour of polymer surface with responsive polymer brushes. *Langmuir* **19**, 8077–8085 (2003).
- Liu, Z. S. & Calvert, P. Multilayer hydrogels as muscle-like actuators. *Adv. Mater.* **12**, 288–291 (2000).
- Anker, J. N. *et al.* Biosensing with plasmonic nanosensors. *Nature Mater.* **7**, 442–453 (2008).
- Tokarev, I. & Minko, S. Stimuli-responsive hydrogel thin films. *Soft Matter* **5**, 511–524 (2009).
- Koberstein, J. T. Molecular design of functional polymer surfaces. *J. Polym. Sci. Pol. Phys.* **42**, 2942–2956 (2004).
- Carey, D. H., Grunzinger, S. J. & Ferguson, G. S. Entropically influenced reconstruction at the PBD-ox/water interface: The role of physical crosslinking and rubber elasticity. *Macromolecules* **33**, 8802–8812 (2000).
- Draper, J., Luzinov, I., Minko, S., Tokarev, I. & Stamm, M. Mixed polymer brushes by sequential polymer addition: Anchoring layer effect. *Langmuir* **20**, 4064–4075 (2004).
- Motornov, M. *et al.* Stimuli-responsive colloidal systems from mixed brush-coated nanoparticles. *Adv. Funct. Mater.* **17**, 2307–2314 (2007).
- Abu-Lail, N. I., Kaholek, M., LaMattina, B., Clark, R. L. & Zauscher, S. Micro-cantilevers with end-grafted stimulus-responsive polymer brushes for actuation and sensing. *Sensor. Actuat. B-Chem.* **114**, 371–378 (2006).
- Ayres, N., Cyrus, C. D. & Brittain, W. J. Stimuli-responsive surfaces using polyampholyte polymer brushes prepared via atom transfer radical polymerization. *Langmuir* **23**, 3744–3749 (2007).
- Azzaroni, O., Brown, A. A. & Huck, W. T. S. UCST wetting transitions of polyzwitterionic brushes driven by self-association. *Angew. Chem. Int. Ed.* **45**, 1770–1774 (2006).
- Santer, S., Kopyshv, A., Donges, J., Yang, H. K. & Ruhe, J. Dynamically reconfigurable polymer films: Impact on nanomotion. *Adv. Mater.* **18**, 2359–2362 (2006).
- Wu, T. *et al.* Behaviour of surface-anchored poly(acrylic acid) brushes with grafting density gradients on solid substrates: 1. Experiment. *Macromolecules* **40**, 8756–8764 (2007).
- Xu, C. *et al.* Effect of block length on solvent response of block copolymer brushes: Combinatorial study with block copolymer brush gradients. *Macromolecules* **39**, 3359–3364 (2006).
- Motornov, M., Sheparovych, R., Tokarev, I., Roiter, Y. & Minko, S. Nonwetttable thin films from hybrid polymer brushes can be hydrophilic. *Langmuir* **23**, 13–19 (2007).
- Sheparovych, R., Motornov, M. & Minko, S. Adapting low-adhesive thin films from mixed polymer brushes. *Langmuir* **24**, 13828–13832 (2008).
- Sheparovych, R., Motornov, M. & Minko, S. Low adhesive surfaces which adapt changing surrounding environment. *Adv. Mater.* **21**, 1840–1844 (2009).
- Tanaka, T. & Fillmore, D. J. Kinetics of swelling of gels. *J. Chem. Phys.* **70**, 1214–1218 (1979).
- Toomey, R., Freidank, D. & Ruhe, J. Swelling behaviour of thin, surface-attached polymer networks. *Macromolecules* **37**, 882–887 (2004).
- Crowe-Willoughby, J. A. & Genzer, J. Formation and properties of responsive siloxane-based polymeric surfaces with tunable surface reconstruction kinetics. *Adv. Funct. Mater.* **19**, 460–469 (2009).
- Crowe, J. A. & Genzer, J. Creating responsive surfaces with tailored wettability switching kinetics and reconstruction reversibility. *J. Am. Chem. Soc.* **127**, 17610–17611 (2005).
- Tokarev, I., Orlov, M. & Minko, S. Responsive polyelectrolyte gel membranes. *Adv. Mater.* **18**, 2458–2460 (2006).
- Tokarev, I. & Minko, S. Multiresponsive hierarchically structured membranes: new challenging biomimetic materials for biosensors, controlled release, biochemical gates and nanoreactors. *Adv. Mater.* **21**, 241–247 (2009).
- Tokarev, I. *et al.* Stimuli-responsive hydrogel membranes coupled with biocatalytic processes. *ACS Appl. Mater. Interfaces* **3**, 532–536 (2009).
- Decher, G. Fuzzy nanoassemblies: Toward layered polymeric multicomposites. *Science* **277**, 1232–1237 (1997).
- Lvov, Y., Ariga, K., Ichinose, I. & Kunitake, T. Assembly of multicomponent protein films by means of electrostatic layer-by-layer adsorption. *J. Am. Chem. Soc.* **117**, 6117–6123 (1995).
- Decher, G. & Schlenoff, J. B. *Multilayer Thin Films* (Wiley-VCH, 2003).
- Itano, K., Choi, J. Y. & Rubner, M. F. Mechanism of the pH-induced discontinuous swelling/deswelling transitions of poly(allylamine hydrochloride)-containing polyelectrolyte multilayer films. *Macromolecules* **38**, 3450–3460 (2005).
- Kharlampieva, E., Kozlovskaya, V., Tyutina, J. & Sukhishvili, S. A. Hydrogen-bonded multilayers of thermoresponsive polymers. *Macromolecules* **38**, 10523–10531 (2005).
- Hua, F., Cui, T. H. & Lvov, Y. M. Ultrathin cantilevers based on polymer-ceramic nanocomposite assembled through layer-by-layer adsorption. *Nano Lett.* **4**, 823–825 (2004).
- Mertz, D. *et al.* Mechanically responding nanovalves based on polyelectrolyte multilayers. *Nano Lett.* **7**, 657–662 (2007).
- Urban, M. W. Intelligent polymeric coatings; current and future advances. *Polym. Rev.* **46**, 329–339 (2006).
- Misra, A., Jarrett, W. L. & Urban, M. W. Fluoromethacrylate-containing colloidal dispersions: Phospholipid-assisted synthesis, particle morphology, and temperature-responsive stratification. *Macromolecules* **40**, 6190–6198 (2007).
- Motornov, M., Sheparovych, R., Lupitskyy, R., MacWilliams, E. & Minko, S. Superhydrophobic surfaces generated from water-borne dispersions of hierarchically assembled nanoparticles coated with a reversibly switchable shell. *Adv. Mater.* **20**, 200–205 (2008).
- Urban, M. W. Stratification, Stimuli-responsiveness, self-healing, and signalling in polymer networks. *Prog. Polym. Sci.* **34**, 679–687 (2009).
- Andreeva, D. V., Fix, D., Mohwald, H. & Shchukin, D. G. Self-healing anticorrosion coatings based on pH-sensitive polyelectrolyte/inhibitor sandwich-like nanostructures. *Adv. Mater.* **20**, 2789–2794 (2008).
- Bajpai, A. K., Shukla, S. K., Bhanu, S. & Kankane, S. Responsive polymers in controlled drug delivery. *Prog. Polym. Sci.* **33**, 1088–1118 (2008).
- Alexander, C. & Shakesheff, K. M. Responsive polymers at the biology/materials science interface. *Adv. Mater.* **18**, 3321–3328 (2006).
- Lutolf, M. P. *et al.* Synthetic matrix metalloproteinase-sensitive hydrogels for the conduction of tissue regeneration: Engineering cell-invasion characteristics. *Proc. Natl Acad. Sci. USA* **100**, 5413–5418 (2003).
- Alarcon, C. D. H., Farhan, T., Osborne, V. L., Huck, W. T. S. & Alexander, C. Bioadhesion at micro-patterned stimuli-responsive polymer brushes. *J. Mater. Chem.* **15**, 2089–2094 (2005).

47. Ionov, L., Houbenov, N., Sidorenko, A., Stamm, M. & Minko, S. Stimuli-responsive command polymer surface for generation of protein gradients. *Biointerphases* **4**, FA45–FA49 (2009).
48. Hayashi, G., Hagihara, M., Dohno, C. & Nakatani, K. Photoregulation of a peptide-RNA interaction on a gold surface. *J. Am. Chem. Soc.* **129**, 8678–8679 (2007).
49. Ebara, M. *et al.* Temperature-responsive cell culture surfaces enable “on-off” affinity control between cell integrins and RGDS ligands. *Biomacromolecules* **5**, 505–510 (2004).
50. Lue, S. J., Hsu, J. J. & Wei, T. C. Drug permeation modeling through the thermo-sensitive membranes of poly(*N*-isopropylacrylamide) brushes grafted onto micro-porous films. *J. Membrane Sci.* **321**, 146–154 (2008).
51. Motornov, M. *et al.* Switchable selectivity for gating ion transport with mixed polyelectrolyte brushes: approaching ‘smart’ drug delivery systems. *Nanotechnology* **20**, 434006 (2009).
52. Wong, V. N. *et al.* Separation of peptides with polyionic nanosponges for MALDI-MS analysis. *Langmuir* **25**, 1459–1465 (2009).
53. Nagase, K. *et al.* Effects of graft densities and chain lengths on separation of bioactive compounds by nanolayered thermoresponsive polymer brush surfaces. *Langmuir* **24**, 511–517 (2008).
54. Edmondson, S., Frieda, K., Comrie, J. E., Onck, P. R. & Huck, W. T. S. Buckling in quasi-2D polymers. *Adv. Mater.* **18**, 724–728 (2006).
55. Zhou, F., Shu, W. M., Welland, M. E. & Huck, W. T. S. Highly reversible and multi-stage cantilever actuation driven by polyelectrolyte brushes. *J. Am. Chem. Soc.* **128**, 5326–5327 (2006).
56. Valiaev, A., Abu-Lail, N. I., Lim, D. W., Chilkoti, A. & Zauscher, S. Microcantilever sensing and actuation with end-grafted stimulus-responsive elastin-like polypeptides. *Langmuir* **23**, 339–344 (2007).
57. Zhou, F. *et al.* Polyelectrolyte brush amplified electroactuation of microcantilevers. *Nano Lett.* **8**, 725–730 (2008).
58. Singamaneni, S. *et al.* Bimaterial microcantilevers as a hybrid sensing platform. *Adv. Mater.* **20**, 653–680 (2008).
59. Jonas, A. M., Hu, Z. J., Glinel, K. & Huck, W. T. S. Effect of nanoconfinement on the collapse transition of responsive polymer brushes. *Nano Lett.* **8**, 3819–3824 (2008).
60. Lee, W. K., Patra, M., Linse, P. & Zauscher, S. Scaling behaviour of nanopatterned polymer brushes. *Small* **3**, 63–66 (2007).
61. Raynor, J. E., Petrie, T. A., Garcia, A. J. & Collard, D. M. Controlling cell adhesion to titanium: Functionalization of poly[oligo(ethylene glycol)methacrylate] brushes with cell-adhesive peptides. *Adv. Mater.* **19**, 1724–1728 (2007).
62. Howse, J. R. *et al.* Reciprocating power generation in a chemically driven synthetic muscle. *Nano Lett.* **6**, 73–77 (2006).
63. Merlitz, H., He, G. L., Wu, C. X. & Sommer, J. U. Surface instabilities of monodisperse and densely grafted polymer brushes. *Macromolecules* **41**, 5070–5072 (2008).
64. Tokareva, I., Minko, S., Fendler, J. H. & Hutter, E. Nanosensors based on responsive polymer brushes and gold nanoparticle enhanced transmission surface plasmon resonance spectroscopy. *J. Am. Chem. Soc.* **126**, 15950–15951 (2004).
65. Burg, T. P. *et al.* Weighing of biomolecules, single cells and single nanoparticles in fluid. *Nature* **446**, 1066–1069 (2007).
66. Gupta, S. *et al.* Gold nanoparticles immobilized on stimuli responsive polymer brushes as nanosensors. *Macromolecules* **41**, 8152–8158 (2008).
67. Kozlovskaya, V. *et al.* Ultrathin layer-by-layer hydrogels with incorporated gold nanorods as pH-sensitive optical materials. *Chem. Mater.* **20**, 7474–7485 (2008).
68. Podsiadlo, P. *et al.* Exponential growth of LBL films with incorporated inorganic sheets. *Nano Lett.* **8**, 1762–1770 (2008).
69. Jiang, G. Q., Baba, A. & Advincula, R. Nanopatterning and fabrication of memory devices from layer-by-layer poly(3,4-ethylenedioxythiophene)-poly(styrene sulphonate) ultrathin films. *Langmuir* **23**, 817–825 (2007).
70. Mitamura, K., Imae, T., Tian, S. & Knoll, W. Surface plasmon fluorescence investigation of energy-transfer-controllable organic thin films. *Langmuir* **24**, 2266–2270 (2008).
71. Hilt, J. Z., Gupta, A. K., Bashir, R. & Peppas, N. A. Ultrasensitive biomems sensors based on microcantilevers patterned with environmentally responsive hydrogels. *Biomed. Microdevices* **5**, 177–184 (2003).
72. Mack, N. H. *et al.* Optical transduction of chemical forces. *Nano Lett.* **7**, 733–737 (2007).
73. Kang, J. H. *et al.* Thermoresponsive hydrogel photonic crystals by three-dimensional holographic lithography. *Adv. Mater.* **20**, 3061–3065 (2008).
74. Ben-Moshe, M., Alexeev, V. L. & Asher, S. A. Fast responsive crystalline colloidal array photonic crystal glucose sensors. *Anal. Chem.* **78**, 5149–5157 (2006).
75. Jiang, C. Y., Markutsya, S., Pikus, Y. & Tsukruk, V. V. Freely suspended nanocomposite membranes as highly sensitive sensors. *Nature Mater.* **3**, 721–728 (2004).
76. Dong, L., Agarwal, A. K., Beebe, D. J. & Jiang, H. R. Adaptive liquid microlenses activated by stimuli-responsive hydrogels. *Nature* **442**, 551–554 (2006).
77. Hendrikson, G. R. & Lyon, L. A. Bioresponsive hydrogels for sensing application. *Soft Matter* **5**, 29–35 (2009).
78. Sidorenko, A., Krupenkin, T., Taylor, A., Fratzl, P. & Aizenberg, J. Reversible switching of hydrogel-actuated nanostructures into complex micropatterns. *Science* **315**, 487–490 (2007).
79. Kuksenok, O., Yashin, V. V. & Balazs, A. C. Mechanically induced chemical oscillations and motion in responsive gels. *Soft Matter* **3**, 1138–1144 (2007).
80. Discher, D. E. *et al.* Emerging applications of polymersomes in delivery: From molecular dynamics to shrinkage of tumours. *Prog. Polym. Sci.* **32**, 838–857 (2007).
81. Blanazs, A., Armes, S. P. & Ryan, A. J. Self-assembled block copolymer aggregates: From micelles to vesicles and their biological applications. *Macromol. Rapid Comm.* **30**, 267–277 (2009).
82. Qi, L., Chapel, J. P., Castaing, J. C., Fresnais, J. & Berret, J. F. Organic versus hybrid coacervate complexes: co-assembly and adsorption properties. *Soft Matter* **4**, 577–585 (2008).
83. Yan, Y. *et al.* Hierarchical self-assembly in solutions containing metal ions, ligand, and diblock copolymer. *Angew. Chem. Int. Ed.* **46**, 1807–1809 (2007).
84. Voets, I. K. *et al.* Spontaneous symmetry breaking: formation of Janus micelles. *Soft Matter* **5**, 999–1005 (2009).
85. Li, M. H. & Keller, P. Stimuli-responsive polymer vesicles. *Soft Matter*, **5**, 927–937 (2009).
86. Chiu, H. C., Lin, Y. W., Huang, Y. F., Chuang, C. K. & Chern, C. S. Polymer vesicles containing small vesicles within interior aqueous compartments and pH-responsive transmembrane channels. *Angew. Chem. Int. Ed.* **47**, 1875–1878 (2008).
87. Oh, J. K., Drumright, R., Siegwart, D. J. & Matyjaszewski, K. The development of microgels/nanogels for drug delivery applications. *Prog. Polym. Sci.* **33**, 448–477 (2008).
88. Morimoto, N., Qiu, X. P., Winnik, F. M. & Akiyoshi, K. Dual stimuli-responsive nanogels by self-assembly of polysaccharides lightly grafted with thiol-terminated poly(*N*-isopropylacrylamide) chains. *Macromolecules* **41**, 5985–5987 (2008).
89. Morimoto, N., Winnik, F. M. & Akiyoshi, K. Botryoidal assembly of cholesteryl-pullulan/poly(*N*-isopropylacrylamide) nanogels. *Langmuir* **23**, 217–223 (2007).
90. Motornov, M. *et al.* “Chemical transformers” from nanoparticle ensembles operated with logic. *Nano Lett.* **8**, 2993–2997 (2008).
91. Donath, E., Sukhorukov, G. B., Caruso, F., Davis, S. A. & Möhwald, H. Novel hollow polymer shells by colloid-templated assembly of polyelectrolytes. *Angew. Chem. Int. Ed.* **37**, 2202–2205 (1998).
92. Zelikin, A. N., Li, Q. & Caruso, F. Disulphide-stabilized poly(methacrylic acid) capsules: Formation, crosslinking, and degradation behaviour. *Chem. Mater.* **20**, 2655–2661 (2008).
93. Levy, T., Dejugnat, C. & Sukhorukov, G. B. Polymer microcapsules with carbohydrate-sensitive properties. *Adv. Funct. Mater.* **18**, 1586–1594 (2008).
94. Kozlovskaya, V., Kharlampieva, E., Mansfield, M. L. & Sukhishvili, S. A. Poly(methacrylic acid) hydrogel films and capsules: Response to pH and ionic strength, and encapsulation of macromolecules. *Chem. Mater.* **18**, 328–336 (2006).
95. Edwards, E. W., Chanana, M., Wang, D. & Möhwald, H. Stimuli-responsive reversible transport of nanoparticles across water/oil interfaces. *Angew. Chem. Int. Ed.* **47**, 320–323 (2008).
96. Binks, B. P., Murakami, R., Armes, S. P. & Fujii, S. Temperature-induced inversion of nanoparticle-stabilized emulsions. *Angew. Chem. Int. Ed.* **44**, 4795–4798 (2005).
97. Binks, B. P. & Murakami, R. Phase inversion of particle-stabilized materials from foams to dry water. *Nature Mater.* **5**, 865–869 (2006).
98. Lu, Y., Mei, Y., Drechsler, M. & Ballauff, M. Thermosensitive core-shell particles as carriers for Ag nanoparticles: Modulating the catalytic activity by a phase transition in networks. *Angew. Chem. Int. Ed.* **45**, 813–816 (2006).
99. Lu, Y. *et al.* Thermosensitive core-shell microgel as a “nanoreactor” for catalytic active metal nanoparticles. *J. Mater. Chem.* **19**, 3955–3961 (2009).
100. Skirtach, A. G. *et al.* Laser-induced release of encapsulated materials inside living cells. *Angew. Chem. Int. Ed.* **45**, 4612–4617 (2006).
101. Kreft, O., Javier, A. M., Sukhorukov, G. B. & Parak, W. J. Polymer microcapsules as mobile local pH-sensors. *J. Mater. Chem.* **17**, 4471–4476 (2007).
102. Gillies, E. R., Jonsson, T. B. & Frechet, J. M. J. Stimuli-responsive supramolecular assemblies of linear-dendritic copolymers. *J. Am. Chem. Soc.* **126**, 11936–11943 (2004).
103. Laugel, N. *et al.* Relationship between the growth regime of polyelectrolyte multilayers and the polyanion/polycation complexation enthalpy. *J. Phys. Chem. B* **110**, 19443–19449 (2006).

104. Kakizawa, Y. & Kataoka, K. Block copolymer micelles for delivery of gene and related compounds. *Adv. Drug Deliver. Rev.* **54**, 203–222 (2002).
105. Oishi, M., Hayashi, H., Michihiro, I. D. & Nagasaki, Y. Endosomal release and intracellular delivery of anticancer drugs using pH-sensitive PEGylated nanogels. *J. Mater. Chem.* **17**, 3720–3725 (2007).
106. Lee, E. S., Kim, D., Youn, Y. S., Oh, K. T. & Bae, Y. H. A virus-mimetic nanogel vehicle. *Angew. Chem. Int. Ed.* **47**, 2418–2421 (2008).
107. Zhulina, E. B., Singh, C. & Balazs, A. C. Forming patterned films with tethered diblock copolymers. *Macromolecules* **29**, 6338–6348 (1996).
108. Roan, J. R. Soft nanopolyhedra as a route to multivalent nanoparticles. *Phys. Rev. Lett.* **96**, 248301 (2006).
109. Müller, M. Phase diagram of a mixed polymer brush. *Phys. Rev. E* **65**, 30802 (2002).
110. Wenning, L., Müller, M. & Binder, K. How does the pattern of grafting points influence the structure of one-component and mixed polymer brushes? *Europhys. Lett.* **71**, 639–645 (2005).
111. Yin, Y. H. *et al.* A simulated annealing study of diblock copolymer brushes in selective solvents. *Macromolecules* **40**, 5161–5170 (2007).
112. Matsen, M. W. The standard Gaussian model for block copolymer melts. *J. Phys. Condens. Matter.* **14**, R21–R47 (2002).
113. Müller-Plathe, F. Coarse-graining in polymer simulation: From the atomistic to the mesoscopic scale and back. *Chemphyschem* **3**, 754–769 (2002).
114. Praprotnik, M., Delle Site, L. & Kremer, K. Multiscale simulation of soft matter: From scale bridging to adaptive resolution. *Annu. Rev. Phys. Chem.* **59**, 545–571 (2008).
115. Merlitz, H., He, G. L., Sommer, J. U. & Wu, C. H. Reversibly switchable polymer brushes with hydrophobic/hydrophilic behaviour: A Langevin dynamics study. *Macromolecules* **42**, 445–451 (2009).
116. Fang, F. & Szeleifer, I. Controlled release of proteins from polymer-modified surfaces. *Proc. Natl Acad. Sci. USA* **103**, 5769–5774 (2006).
117. Szeleifer, I. & Carignano, M. A. Tethered polymer layers: phase transitions and reduction of protein adsorption. *Macromol. Rapid Comm.* **21**, 423–448 (2000).
118. Israels, R., Leermakers, F. A. M. & Fleer, G. J. On the theory of grafted weak polyacids. *Macromolecules* **27**, 3087–3093 (1994).
119. Ye, Y., McCoy, J. D. & Curro, J. G. Application of density functional theory to tethered polymer chains: Effect of intermolecular attractions. *J. Chem. Phys.* **119**, 555–564 (2003).
120. Ren, C. L., Nap, R. J. & Szeleifer, I. The role of hydrogen bonding in tethered polymer layers. *J. Phys. Chem. B* **112**, 16238–16248 (2008).
121. Zhulina, E. B. & Leermakers, F. A. M. A self-consistent field analysis of the neurofilament brush with amino-acid resolution. *Biophys. J.* **93**, 1421–1430 (2007).
122. Tagliacucchi, M., Calvo, E. J. & Szeleifer, I. Molecular theory of chemically modified electrodes by redox polyelectrolytes under equilibrium conditions: Comparison with experiment. *J. Phys. Chem. C* **112**, 458–471 (2008).
123. Tagliacucchi, M., Calvo, E. J. & Szeleifer, I. Redox and acid base coupling in ultrathin polyelectrolyte films. *Langmuir* **24**, 2869–2877 (2008).
124. Mendez, S., Curro, J. G., McCoy, J. D. & Lopez, G. P. Computational modeling of the temperature-induced structural changes of tethered poly(*N*-isopropylacrylamide) with self-consistent field theory. *Macromolecules* **38**, 174–181 (2005).
125. Wang, Q. Internal structure and charge compensation of polyelectrolyte multilayers: a numerical study. *Soft Matter* **5**, 413–424 (2009).
126. Pattanayek, S. K. & Pereira, G. G. Shape of micelles formed from strongly adsorbed grafted polymers in poor solvents. *Macromol. Theor. Simul.* **14**, 347–357 (2005).
127. Netz, R. R. & Andelman, D. Neutral and charged polymers at interfaces. *Phys. Rep.* **380**, 1–95 (2003).
128. Wang, J. & Müller, M. Microphase separation of diblock copolymer brushes in selective solvents: Single-chain-in-mean-field simulations and integral geometry analysis. *Macromolecules* **42**, 2251–2264 (2009).
129. Groot, R. D. & Warren, P. B. Dissipative particle dynamics: Bridging the gap between atomistic and mesoscopic simulation. *J. Chem. Phys.* **107**, 4423–4435 (1997).
130. Daoulas, K. Ch. & Müller, M. Comparison of simulations of lipid membranes with membranes of block copolymers. *Adv. Polym. Sci.* **224**, 197–233 (2009).
131. Santer, S. *et al.* Memory of surface patterns in mixed polymer brushes: Simulation and experiment. *Langmuir* **23**, 279–285 (2007).
132. Santer, S., Kopyshv, A., Donges, J., Yang, H. K. & Rühle, J. Domain memory of mixed polymer brushes. *Langmuir* **22**, 4660–4667 (2006).
133. Tam, T. K., Ornatska, M., Pita, M., Minko, S. & Katz, E. Polymer brush-modified electrode with switchable and tunable redox activity for bioelectronic applications. *J. Phys. Chem. C* **112**, 8438–8445 (2008).
134. Motornov, M. *et al.* Integrated multifunctional nanosystem from command nanoparticles and enzymes. *Small* **5**, 817–820 (2009).
135. Maye, M. M., Nykpanchuk, Cuisinier, M., van der Lelie, D. & Gang, O. *Nature Mater.* **8**, 388–391 (2009).
136. Ghosh, B. & Urban, M. W. Self-repairing oxetane-substituted chitosan polyurethane networks. *Science* **323**, 1458–1460 (2009).

Acknowledgements

The research was supported by National Science Foundation (grants DMR-0706209, DMR-0602528, DMR-0518785, DMR-0756273; CBET-0756461, CBET-0650705, CBET-0756457, CBET-0756461, CBET-0828046, CBET-0946615, CMMI-0825832, CMMI-0826067 and CMMI-0825773), US ARO (W911NF-05-1-0339), AFOSR-FA9550-08-1-0446 and the US Department of Energy (DE-SC52-06NA27341 and DE-FG02-09ER46604) and the Deutsche Forschungsgemeinschaft (Mu 1674/4).

Additional information

The authors declare no competing financial interests.

Martien A. Cohen Stuart¹, Wilhelm T. S. Huck², Jan Genzer³, Marcus Müller⁴, Christopher Ober⁵, Manfred Stamm⁶, Gleb B. Sukhorukov⁷, Igal Szeleifer⁸, Vladimir V. Tsukruk⁹, Marek Urban¹⁰, Françoise Winnik¹¹, Stefan Zauscher¹², Igor Luzinov^{13†} and Sergiy Minko^{14†}

¹Laboratory of Physical Chemistry and Colloid Science, Wageningen University, Dreijenplein 6, 6703 HB Wageningen, The Netherlands, ²Melville Laboratory for Polymer Synthesis, Department of Chemistry, University of Cambridge, Lensfield Road, Cambridge, CB2 1EW, UK, ³Department of Chemical and Biomolecular Engineering, North Carolina State University, Raleigh, North Carolina 27695, USA, ⁴Institut für Theoretische Physik, Georg-August-Universität, Friedrich-Hund-Platz 1, D 37077 Göttingen, Germany, ⁵Department of Materials Science & Engineering, Cornell University, 310 Bard Hall, Ithaca, New York 14853, USA, ⁶Leibniz-Institut für Polymerforschung Dresden e.V., Hohe Straße 6, 01069 Dresden, Germany, ⁷School of Engineering and Materials Science, Queen Mary University of London, Mile End Road, London, E1 4NS, UK, ⁸Department of Biomedical Engineering, Northwestern University, 2145 Sheridan Road, Evanston, Illinois 60208, USA, ⁹School of Materials Science and Engineering, Georgia Institute of Technology, 771 Ferst Drive, Atlanta, Georgia 30332-0245, USA, ¹⁰School of Polymers and High Performance Materials, University of Southern Mississippi, 118 College Drive, Hattiesburg, Mississippi 39406, USA, ¹¹Faculty of Pharmacy and Department of Chemistry, Université de Montreal, CP 6128 Succursale Centre, Ville Montreal, Quebec H3C 3J7, Canada, ¹²Department of Mechanical Engineering and Materials Science, Duke University, 144 Hudson Hall, Durham, North Carolina 27708, USA, ¹³School of Materials Science and Engineering, 263 Sistine Hall, Clemson University, Clemson, South Carolina 29634-0971, USA, ¹⁴Department of Chemistry and Biomolecular Science, 8 Clarkson Ave, Clarkson University, Potsdam, New York 13699, USA.

†e-mail: luzinov@clemson.edu; sminko@clarkson.edu